MOLECULAR PHYSICS

10.1126/sciadv.1400185

Quantum unidirectional rotation directly imaged with molecules

Kenta Mizuse,[1]* Kenta Kitano,[2] Hirokazu Hasegawa,[3] Yasuhiro Ohshima[1,4†]

A gas-phase molecular ensemble coherently excited to have an oriented rotational angular momentum has recently emerged as an appropriate microscopic system to illustrate quantum mechanical behavior directly linked to classical rotational motion, which has a definite direction. To realize an intuitive visualization of such a unidirectional molecular rotation, we report high-resolution direct imaging of direction-controlled rotational wave packets in nitrogen molecules. The rotational direction was regulated by a pair of time-delayed, polarization-skewed laser pulses, introducing the dynamic chirality to the system. The subsequent spatiotemporal propagation was tracked by a newly developed Coulomb explosion imaging setup. From the observed molecular movie, time-dependent detailed nodal structures, instantaneous alignment, angular dispersion, and fractional revivals of the wave packet are fully characterized while the ensemble keeps rotating in one direction. The present approach, providing an accurate view on unidirectional rotation in quantum regime, will guide more sophisticated molecular manipulations by utilizing its capability in capturing highly structured spatiotemporal evolution of molecular wave packets.

INTRODUCTION

Similar to a three-dimensional (3D) object in a macroscopic scale, molecules can rotate around an arbitrary axis that passes through their center of mass. The rotational period of molecules is typically within the picosecond time regime, at least six orders of magnitude faster than that of the macroscopic counterparts. Such an ultrafast motion of molecules is governed by the physical laws in microscopic scale, that is, quantum mechanics, owing to the size of molecules well below the nanometer range. To gain a detailed insight into the molecular quantum rotation, direct visualization of the ultrafast molecular rotation has been repeatedly carried out for more than a decade by using intense ultrafast laser technology coupled with ion-imaging measurements (*1*–*4*). These observations have manifested quantum mechanical signatures, such as nodal structures and revivals in time-dependent molecular axis probability distribution (*1*–*7*). It has to be noted, however, that the excitation scheme implemented therein kept the projection (here denoted J_z) of the rotational angular momentum onto an arbitrary space-fixed axis in the initial expectation value ($\langle J_z \rangle = 0$) for isotropic distribution. The rotational wave packet thus created cannot be directly linked to any classical rotational motion, which is characterized by a definite sense of rotation.

There have been several proposals and experimental verification of the creation of rotational wave packets with gaining nonzero $\langle J_z \rangle$ value (*8*–*22*). The ways to create such an unidirectionally rotating wave packet include "optical centrifuge" with gradually accelerating circularly rotating laser polarization field (*8*–*14*), implementation with a pair of time-delayed linearly polarized ultrashort laser pulses with skewed mutual polarization direction (*7*, *15*–*19*), and excitation with a chiral train of laser pulses (*20*–*22*). The sense of rotation of the molecular systems has been monitored mostly via spectroscopic probes observing, for example, circular dichroism in the ultraviolet transition (*13*, *16*, *20*, *21*), rotational Doppler effect (*18*), and polarization-controlled coherent Raman signals (*12*). Recently, ion-imaging experiments have been conducted to track the unidirectional rotation of a molecular ensemble (*14*, *19*). They succeeded in capturing some signature of one-way rotational motion of the ensemble, yet its observation window was limited and the angular resolution was relatively low (*14*), or an important character of wave nature, for example, multinodal structure, did not seem to be observed (*19*). Full spatiotemporal evolution of unidirectional rotational wave packet still remains to be explored for further understanding on molecular rotational dynamics.

Here, we report our results on detailed tracking of a spatiotemporal behavior of a unidirectionally rotating ensemble of adiabatically cooled N_2 molecules. Coulomb explosion imaging (*1*–*3*, *23*) has been used to measure the time-dependent orientation of molecules by using a specially designed 2D ion-imaging configuration, which allows us to record fragment ion distribution that cannot be collected by a conventional 2D ion-imaging setup (*23*). We observed that the orientation distribution was intricately dispersed and then revived while rotating in a defined direction as it evolved in time. This is a clear signature of multilevel quantum interference within unidirectionally rotating wave packets (*14*), which has not been visualized so far. The present approach provides us a sharp image of the unidirectionally rotating molecules in quantum regime, and it will also serve as a fundamental diagnostic tool when rotational wave packets are used in broader chemical, physical, or optical applications (*11*, *18*, *24*–*36*).

RESULTS

Figure 1 shows a schematic of the experimental setup, indicating the space-fixed axis system adopted herein. The ensemble of N_2 molecules at the estimated rotational temperature of 6 K has been taken as a sample to be examined (see Materials and Methods). Most of the molecules were populated in the lowest rotational levels with two different nuclear spin wave functions pertinent to two identical ^{14}N nuclei, that is, $J = 0$ for the ortho state ($I_N = 0$ and 2) and $J = 1$ for the para state ($I_N = 1$). To

[1]Institute for Molecular Science, National Institutes of Natural Sciences and SOKENDAI (The Graduate University for Advanced Studies), Okazaki 444-8585, Japan. [2]Department of Physics and Mathematics, Aoyama Gakuin University, Sagamihara, Kanagawa 252-5258, Japan. [3]Department of Basic Science, Graduate School of Arts and Sciences, The University of Tokyo, Tokyo 153-8902, Japan. [4]Department of Chemistry, Graduate School of Science and Engineering, Tokyo Institute of Technology, Tokyo 152-8550, Japan.
*Present address: Department of Chemistry, Graduate School of Science and Engineering, Tokyo Institute of Technology, Tokyo 152-8550, Japan.
†Corresponding author. E-mail: ohshima@chem.titech.ac.jp

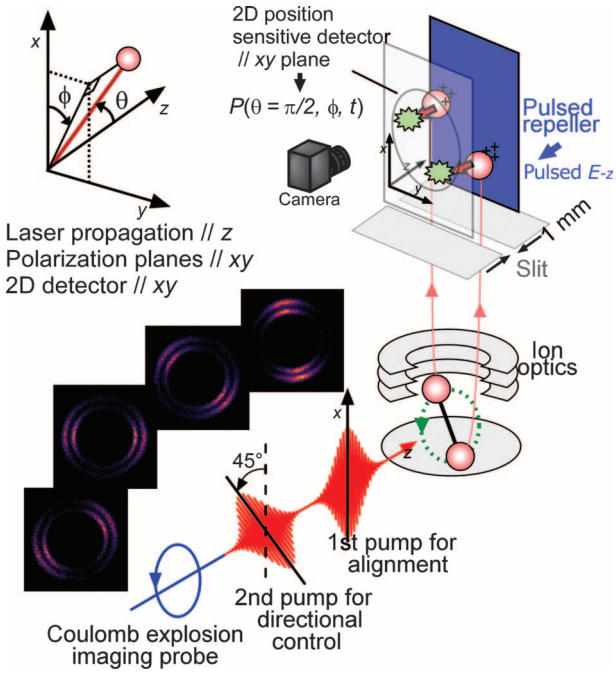

Fig. 1. Schematic of experimental setup and the space-fixed axis system used. The upper-left image shows the definition of the present space-fixed axis system, in which the laser propagates toward the *z* direction and the polarization of the first pulse is parallel to the *y* axis. All the electric field vectors of the three pulses are in the *xy* plane. The polar angle is θ, and the azimuthal angle is ϕ. Because the laser polarizations define the plane of rotation, in this case, time dependence with respect to ϕ in the *xy* plane characterizes unidirectional rotation dynamics. The apparatus consists of ion optics (a set of gridless lens electrodes), a mechanical slit, a pulsed repeller, and a 2D position sensitive detector (MCP/screen/camera). The detector surface is parallel to the *xy* plane so that the angle ϕ of the ejected direction for the Coulomb exploded fragments can be directly measured from the 2D image. The four insets show typical observed images of the fragment ions (after the calibration to make the images circles).

induce unidirectional rotation in the sample, a pair of time-delayed, polarization-skewed linearly polarized pulses was irradiated onto it, as was in the previous studies (*7*, *15*–*19*). The subsequent dynamics was followed by recording the time-dependent angular probability distribution with Coulomb explosion imaging induced by the third, circularly polarized probe pulse. The present ion-imaging setup directly provided us the cross section of the distribution in the *xy* plane (see Materials and Methods). To demonstrate the capability of the setup, some results for single-pump experiments are indicated in Fig. 2. Here, the single *y*-polarized pump pulse followed by the probe pulse was adopted to image the conventional nonadiabatic molecular alignment (*1*–*7*). Observed N^{3+} ion images and the corresponding polar plots at several delay times are indicated. At the half revival, t = 4.0 ps ~ $T_{rev}/2$, where $T_{rev} = 1/(2cB) \approx 8.38$ ps is the full revival time with B (=1.989581 cm^{-1}) being the rotational constant of the N_2 molecule (*3*), an elongated "figure 8" shape appears, which corresponds to the highest degree of alignment (the center images of Fig. 2). This timing is set exclusively to the interval between the two pump pulses in the following three pulse experiments. We note that the quality of the images taken in the present study is much improved than that in the previous report (*3*).

As the results of the three pulse experiments, the observed time-dependent distribution for the unidirectional rotation is represented in a false-color 2D plot (Fig. 3A), where the horizontal axis corresponds to the delay time, *t*, of the explosion probe against the first pulse, whereas the vertical axis corresponds to the azimuthal angle, ϕ, defined in Fig. 1. The peak intensity of the first and the second pulses was estimated to be 30 TW/cm^2 in this case from the experimental parameters, that is, beam spot size, pulse duration, and pulse energy. Before t = 0, molecules are randomly oriented and the distribution is isotropic (constant against azimuthal angle, with a value of $1/4\pi$). Then, the first alignment pulse induces the well-known nonadiabatic molecular alignment (*1*–*7*), and its symmetric dynamics with respect to the horizontal lines at 180° continues until the second pulse comes. The second, tilted pulse is introduced at around the half revival, t = 4.0 ps. This symmetrically aligned wave packet (Fig. 2, center) is exerted by the torque via the interaction with the skewed second pulse to induce unidirectional

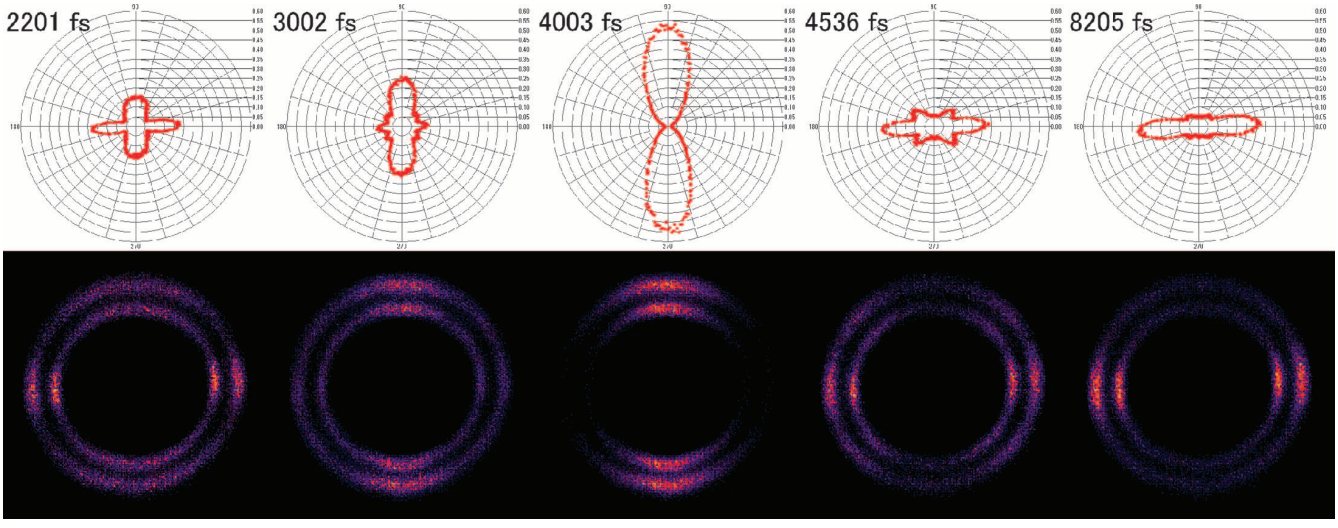

Fig. 2. Selected snapshots of rotational wave packet dynamics induced by a single linearly polarized pulse. (**Bottom**) Observed N^{3+} ion images (after the calibration). The double ring structure comes from the two channels of Coulomb explosion (N^{3+} from N_2^{4+} and N_2^{5+}), in which higher-charge states lead to larger kinetic energy release (outer ring). (**Top**) Polar plots of the observed angular probability. The polarization of the pulse is vertical in this figure.

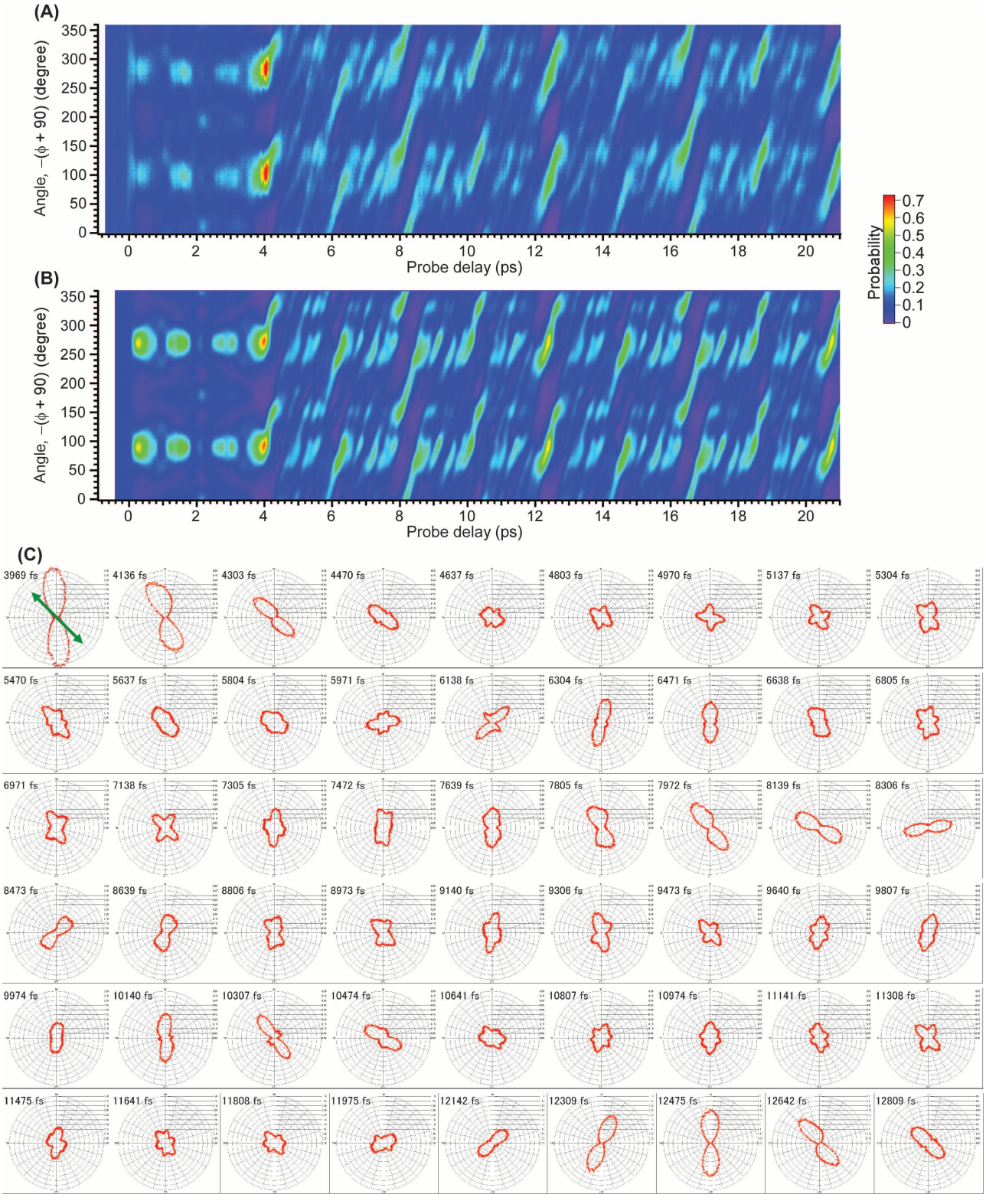

Fig. 3. Time-dependent angular distributions and selected snapshots of unidirectional molecular rotation. (**A**) Observed time- and angular-dependent probability, $P(\theta = \pi/2,\phi,t)$, in the rotational wave packet dynamics. Before $t = 0$, molecules are randomly oriented and therefore the probability is just $1/4\pi \sim 0.08$. (**B**) Simulated plot corresponding to (A), with the laser intensity set to 15 TW/cm^2. (**C**) Polar plots of the observation in (A), in which the probability is displayed as a radius from the origin. The plots show the dynamics in the *xy* plane, and the first pulse polarization is vertical, whereas the second is tilted 45° to the left. Selected snapshots during the revival time, T_{rev}, after the second pulse irradiation are shown.

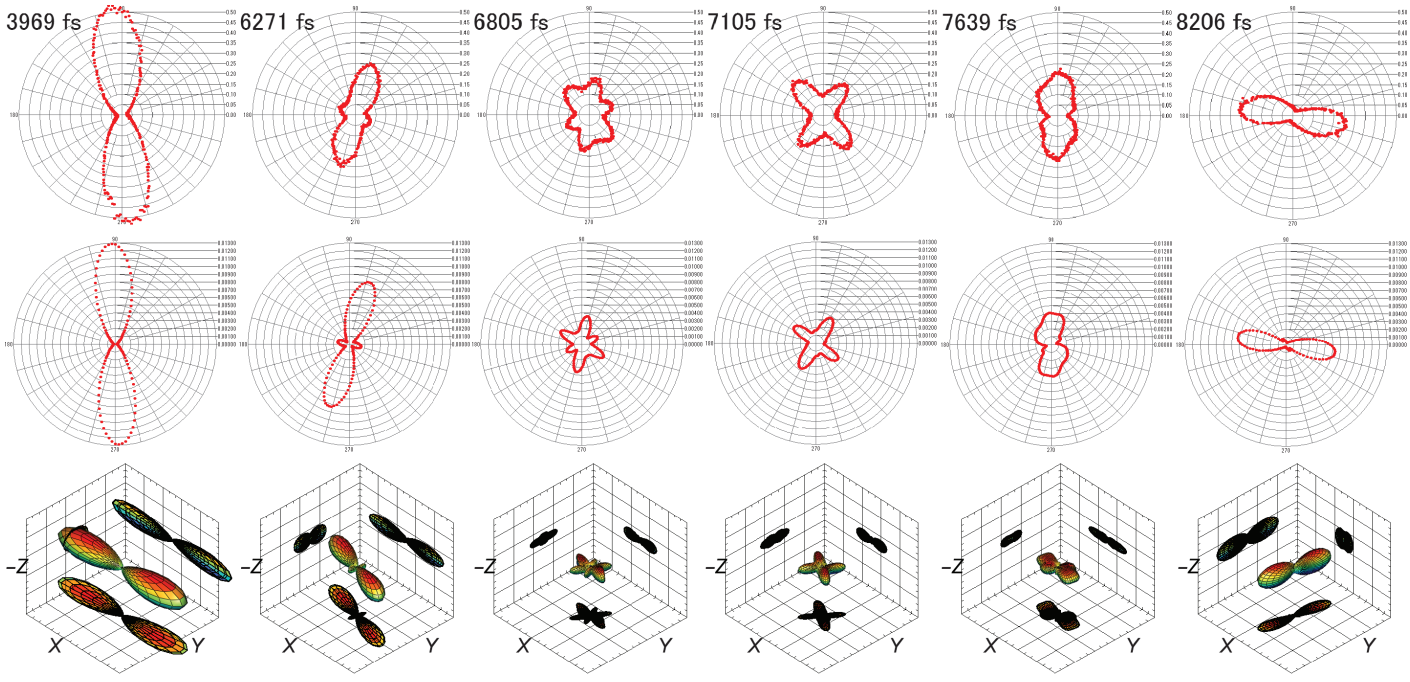

Fig. 4. Comparison of experimental and theoretical wave packet dynamics. (**Top**) Observed angular distribution, same as in Fig. 2C. (**Middle**) Simulated polar plots. (**Bottom**) Simulated 3D probability distribution of the wave packet and their projections onto the three planes.

rotation (counterclockwise in this case). The following dynamics appears as inclined traces in Fig. 3A afterward. The oblique plot ($t >$ 4.0 ps) clearly shows revivals after the interval of T_{rev}, as does the nonadiabatic molecular alignment with a single linearly polarized pulse (*1*–*7*). The traces correspond to the time evolution of the most probable angle, and their slopes give us an effective period of ~2 ps for the 2π rotation. This value correlates to the classical angular speed of a rotating N_2 molecule having an angular momentum of ~ $4\hbar$. The observed plot (Fig. 3A) has been simulated by the numerical calculation (see Materials and Methods). Because the results are quite sensitive to the peak intensity of the pulses, it was optimized to reproduce the observation, whereas the other parameters, for example, rotational temperature and pulse duration, were fixed to the experimental values. The resultant simulated plot (Fig. 3B) satisfactorily reproduces the observed one, indicating the validity of the measurements. The optimized peak intensity (15 TW/cm^2) is half of the experimentally estimated value.

For a more detailed discussion on dynamics, selected snapshots of the angular distribution are displayed in Fig. 3C. It is evident that the distribution rotates in the counterclockwise direction when the time course of the plots is followed, in particular, just after the interaction with the skewed pulse (t ~ 4 ps). From the symmetrical "figure 8" shape (Fig. 2, center), the distribution is distorted to be of "propeller" shape (the first three plots in Fig. 3C). It is asymmetric with respect to any line passing the center, indicating the transient chiral nature of the system. As the system evolves in time, the "propeller" is further deformed into a cross-like structure at ~1 and ~3 ps after the creation of the unidirectionally rotating wave packet. These timings are near $T_{rev}/8$ and $3T_{rev}/8$, respectively, and the transformation of the distribution is regarded as the wave packet dispersion (*14*). An analysis by the Fourier transformation of the multiple moments, $\langle P_n(\cos\phi)\rangle$, where P_n is an nth-degree Legendre polynomial, shows, and the numerical calculation confirms, that the wave packets created herein mainly consist of rotational states with J up to 8 (fig. S1). Then, multiple angular speed components coexist, and after the instantaneous alignment (with the "figure 8" shape), the angular distribution starts dispersing, resulting in the "cross" or more complicated shapes shown in the polar snapshots. In such a cross-shaped distribution, two opposed arms correspond to the slower components and the other two arms correspond to the faster ones. After the angular dispersion, the faster arms catch up with the slower ones, and the alignment revives at $T_{rev}/4$, $3T_{rev}/4$, and so on (t ~6 and 8 ps, for example). The angular dispersion and the revival are a manifestation of the quantum nature of a rotational wave packet (*14*), and it is directly observed in the unidirectional rotation for the first time in the present study. In Fig. 4, some of the observed polar plots are compared with the results from the numerical calculation, with the corresponding 3D snapshots from the calculation. The simulated snapshots reasonably agree with the observed ones. The animated angular distribution from the observation and the simulation (movies S1 and S2) provide full details of the spatiotemporal evolution of the unidirectionally rotating wave packet.

In the 3D snapshots of Fig. 4, distribution along the z direction looks confined to the xy plane as predicted in the previous theoretical study (*15*). This fact is confirmed experimentally by monitoring the integrated signal intensity about the ϕ angle. The time-dependent total signal counts are plotted in fig. S2. In the case of the single-pulse excitation, the signal shows remarkable oscillating features. On the other hand, in the double-pulse unidirectional cases, such an oscillation is damped by the second pulse irradiation, indicating the confined dynamics along the z axis.

We also made measurements with the reduced peak intensity of the first and the second pulses by a factor of 1/2. The observed time-dependent distribution (Fig. 5A) is drastically changed from that

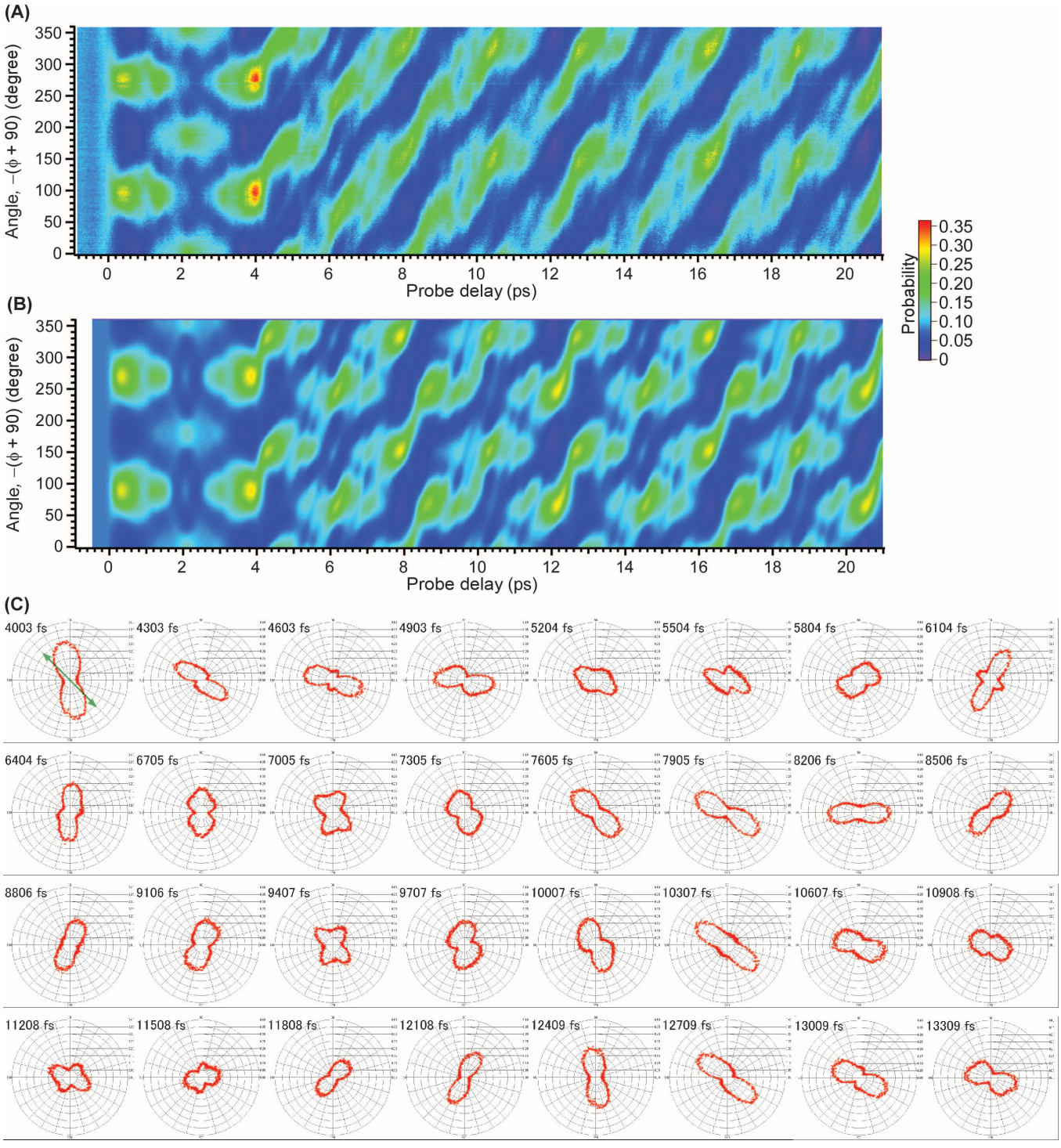

Fig. 5. Time-dependent angular distributions and selected snapshots of unidirectional molecular rotation induced by weaker pulses. (**A**) Observed time- and angular-dependent probability, $P(\theta = \pi/2,\phi,t)$. (**B**) Simulated plot corresponding to (A), with the laser intensity set to 7.5 TW/cm^2. (**C**) Polar plots of the observation in (A).

recorded with the higher intensity (Fig. 3A). The traces in Fig. 5A show more gentle slopes than those in Fig. 3A. An effective period for 2π rotation is derived as ~3.5 ps, and the corresponding angular speed correlates to an angular momentum of ~$2\hbar$. This corroborates with the lower degree of rotational excitation (mainly up to $J = 4$) in the created wave packet (fig. S3). The broadness of the traces is also explained by the

lower degree of excitation, which leads to a less confined angular distribution in the wave packet. The simulated results (Fig. 5B) with the peak intensity of 7.5 TW/cm^2 satisfactorily reproduce the observation (Fig. 5A). Detailed time evolution is also significantly altered, as shown in the selected snapshots of the observed distribution (Fig. 5C) and the movie of all the observed time dependence (movie S3). The wave packet dispersion at $T_{rev}/8$ after the creation of the unidirectionally rotating wave packet is less remarkable, and the "propeller" shape of the distribution is mostly preserved throughout the time evolution. This behavior can be regarded as the approaching of a dispersing wave packet toward a nondispersing wave packet, which resembles the classical rotation, as in a recent observation (*14*).

DISCUSSION

The present detailed observation of the highly structured spatiotemporal evolution of the unidirectionally rotating wave packets mostly relies on the successful restriction of most of the initial state to the lowest rotational levels, $J = 0$ and 1, for the ortho and para nuclear spin isomers of N_2, respectively. Here, the dispersion and revival of the wave packet are clearly imaged. Recently, Lin *et al.* (*19*) have also reported an independent experimental observation of unidirectionally rotating N_2 molecules by coincidence ion imaging. The angular distribution reported therein, however, was much less structured, and its time evolution looked gradual and modest. This is because the molecular ensemble studied in (*19*) was at higher temperature (20 K), and the ensemble average over many initial states smeared out the fine interference structure.

In our experiments mentioned earlier, counterclockwise unidirectional rotation (that is, ϕ-increasing direction) was induced by setting the second pump pulse tilted by 45° to the left to the first pulse (that is, $\Delta\phi = \pi/4$). To make clockwise (ϕ-decreasing) rotation, the simplest way is just exchanging the polarization of the two pulses ($\Delta\phi = -\pi/4$) while keeping the delay between them the same for maximum alignment (*15*–*17*). Alternatively, the delay may be set for maximum anti-alignment (for example, at ~8.2 ps, as shown in Fig. 2) while keeping the mutual polarization ($\Delta\phi = \pi/4$) (*16*). The situation was experimentally verified in (*19*).

Various (potential) applications of the field-free molecular alignment and manipulated rotational wave packets have been reported in studies of physicochemical processes (*24*–*30*), information processing (*31*–*34*), and advanced optics (*18*, *35*, *36*). In particular, unidirectionally rotating molecular gas ensembles have been expected to be used as broadband, transient wave plate retarders owing to the rotating birefringence of the system (*35*). Such a novel optics would lead to much more sophisticated polarization shaping of ultrafast light pulses. In addition, counter-rotating wave packets of two different nuclear spin isomers of a molecule and a nondispersing unidirectional rotational wave packet ("quantum cogwheel") will be beneficial, respectively, to nuclear spin isomer separation (*15*, *21*) or to precise clocking of two ultrafast pulses from different sources (*34*). For all these application of unidirectional molecular rotation, the experimental evaluation of the target ensemble is essential because the details of instantaneous shape of the angular probability distribution will determine the output. When nonresonant intense ultrashort laser fields are adopted, the excitation process is much deviated from the perturbative regime (*37*), and the resultant state is extremely sensitive to the field intensity, the precise measurement of which is not an easy task. In this respect, the present high-resolution spatiotemporal imaging of the rotational wave packet should be of much significance for further studies. Systematically examining the crossover of a dispersing rotational wave packet to a "quantum cogwheel" would also be of relevance to quantum-classical correspondence. The present high-resolution imaging would be an ideal experimental approach for this objective. When the quality of the observed time-dependent angular distribution is high enough, full experimental reconstruction of the wave packet or, more generally, the density matrix for the final state is feasible (*38*). High-throughput data acquisition of the present ion-imaging setup may fulfill the criteria.

In conclusion, the present Coulomb explosion imaging provides direct tracking of a complex spatiotemporal evolution of unidirectionally rotating wave packets and is a major step toward the full experimental characterization of sculptured molecular quantum states subjected to the coherent interaction with highly controlled laser fields.

MATERIALS AND METHODS

Experimental design

Adiabatically cooled N_2 molecules were introduced to the interaction region of the imaging apparatus, schematically shown in Fig. 1. The rotational temperature of the molecular ensemble was estimated to be 6 K by measuring a rotationally resolved electronic spectrum of NO molecules in the same beam condition (in an independent experiment). At this rotational temperature, the relative population in the rotational states of N_2 was 53, 31, and 15% in $J = 0$, 1, and 2, respectively, and <1% in others. Theoretical simulations based on this initial condition well reproduced the experiments, as mentioned earlier (Figs. 3 to 5). The molecules in the interaction region were irradiated by three femtosecond laser pulses coming from a Ti:sapphire laser amplifier. The first pulse was for molecular alignment (linearly polarized along the *y* axis, center wavelength of 820 nm, 120-fs pulse duration, peak intensity <30 TW/cm^2), the second was for the direction control (a delayed replica of the first one only except for the linear polarization +45° tilted from the *y* axis), and the third was the Coulomb explosion imaging probe (circularly polarized in the *xy* plane, 407 nm, 100 fs, 600 TW/cm^2). Upon the probe pulse irradiation, the sample molecules of all the orientation angle (in the polarization plane) were multiply ionized and then exploded within the laser duration (Coulomb explosion). The direction (left or right) of circular polarization did not affect the observed images. This is because the speed of polarization rotation in 407-nm circularly polarized light is much faster (~1.3 fs per cycle) than the rotational period, and the molecules feel a plane-like laser field. The ejected fragment ion distribution is a direct measure of the molecular axis distribution at the time of probe irradiation. The ions thus created were first accelerated by a set of gridless lens electrodes along the *y* direction, perpendicular to the laser propagation direction, and the 3D expanding ion cloud was sliced out to be a thin disc sharing its center with the sphere by passing through a slit set parallel to the *x* direction. At the time when the sliced ion "sheet" of interest arrived at the new window region, a fast pulsed electric field along the $-z$ direction (~4 kV/cm, ~30-ns rise time) was applied to push it to the 2D position sensitive detector (microchannel plates backed by a phosphor screen and a digital camera), installed parallel to the *xy* plane. The initial ion acceleration by the ion optics results in the compression of spatial expansion in the *y* direction. The raw observed image with an ellipsoidal shape taken by the camera was just calibrated by a multiplying factor to

the y coordinate so that the probe-only image becomes a circle. The corrected image represents a cross section of the fragment ion distribution in the xy plane, that is, $P_{xy}(\phi, t)$. In Coulomb explosion, several dissociation channels of $N_2^{a+} \rightarrow N^{b+} + N^{c+}$ have been observed (*3*, *39*). Because higher charged states are favorable for rapid dissociation before molecular reorientation, we focused the N^{3+} fragment ejected from the $N_2^{4,5+}$ parent as a measure. Because higher charged states are only created in a smaller volume near the beam waist (ca. ~10 μm in diameter), the restricted initial spatial distribution has little effect on the observed images less. In this respect, the present imaging setup can be regarded as in a velocity map configuration, although the focusing of the ion lenses was relatively loose (1-mm distribution at the interaction region corresponds to a ca. 0.50-mm spot at the detector). The first pulse timing was defined as $t = 0$. The second, tilted pump pulse was irradiated with some delay (~4 ps) to the first pulse to apply a torque asymmetrically on the molecular ensemble. The subsequent unidirectional dynamics was observed by scanning the delay of the third, imaging pulse with a 33-fs step. One snapshot typically consists of more than 200,000 ion counts, depending on the timing. Details of our apparatus and data acquisition will be given in a future publication.

Numerical calculation

A model calculation is performed to evaluate the observed time-dependent angular distribution of the molecular axis in the unidirectionally rotating N_2 ensemble. Here, the rotational wave packet, $|\Psi(t)\rangle$, created from an initial rotational state, $|r_i\rangle$, by the two successive pulses is expanded as $|\Psi_{r_i}(t)\rangle = \Sigma_r C_{r_i,r} \exp(-i\omega_r t)|r\rangle$ with $\omega_r = BJ(J+1)/\hbar$. The rotational state, $|r\rangle$, of a diatomic molecule is just a spherical harmonic, $Y_{J,M}(\theta, \phi)$. J and M stand for the rotational angular momentum and its projection onto the space-fixed z axis, and θ and ϕ are the polar and azimuthal angles characterizing the direction of the molecular axis with respect to the space-fixed axis system defined in Fig. 1. The complex expansion coefficient, $C_{r_i,r}$, is derived according to the procedure developed in our previous studies (*16*, *17*), which considered the transformation of the rotational states by the interaction with a pair of time-delayed linearly polarized laser pulses with skewed mutual polarization direction. Then, the time-dependent angular distribution is calculated as $P(\theta, \phi, t) = \Sigma_{r_i} W_{r_i} |\Psi_{r_i}(t)|^2$, where W_{r_i} is the initial population in $|r_i\rangle$, determined by the Boltzmann factor at the temperature of the ensemble and the 1:2 statistical weights for the para ($I_N = 1$ with odd J) and the ortho ($I_N = 0, 2$ with even J) nuclear spin isomers. The observed images correspond to the distribution within the xy plane, that is, $P_{xy}(\phi, t) = P(\theta = \pi/2, \phi, t)$.

SUPPLEMENTARY MATERIALS

Supplementary material for this article is available at http://advances.sciencemag.org/cgi/content/full/1/6/e1400185/DC1

Fig. S1. Fourier transformation analyses of $\langle P_n(\cos\phi)\rangle$ for the higher-intensity experiment.
Fig. S2. Time-dependent signal intensity as a measure of the probability in the xy plane.
Fig. S3. Fourier transformation analyses of $\langle P_n(\cos\phi)\rangle$ for the lower-intensity experiment.
Movie S1. Unidirectional rotation induced by higher-intensity pulses (all frames of Fig. 3).
Movie S2. Calculated unidirectional molecular rotation, corresponding to movie S1.
Movie S3. Experimental movie for the lower-intensity case.

REFERENCES AND NOTES

1. F. Rosca-Pruna, M. Vrakking, Experimental observation of revival structures in picosecond laser-induced alignment of I_2. *Phys. Rev. Lett.* **87**, 153902 (2001).
2. F. Rosca-Pruna, M. J. J. Vrakking, Revival structures in picosecond laser-induced alignment of I_2 molecules. I. Experimental results. *J. Chem. Phys.* **116**, 6567–6578 (2002).
3. P. W. Dooley, I. V. Litvinyuk, K. F. Lee, D. M. Rayner, M. Spanner, D. M. Villeneuve, P. B. Corkum, Direct imaging of rotational wave-packet dynamics of diatomic molecules. *Phys. Rev. A* **68**, 023406 (2003).
4. M. D. Poulsen, E. Péronne, H. Stapelfeldt, C. Z. Bisgaard, S. S. Viftrup, E. Hamilton, T. Seideman, Nonadiabatic alignment of asymmetric top molecules: Rotational revivals. *J. Chem. Phys.* **121**, 783–791 (2004).
5. H. Stapelfeldt, T. Seideman, *Colloquium*: Aligning molecules with strong laser pulses. *Rev. Mod. Phys.* **75**, 543–557 (2003).
6. T. Seideman, E. Hamilton, Nonadiabatic alignment by intense pulses. Concepts, theory, and directions. *Adv. At. Mol. Opt. Phys.* **52**, 289–329 (2006).
7. Y. Ohshima, H. Hasegawa, Coherent rotational excitation by intense nonresonant laser fields. *Int. Rev. Phys. Chem.* **29**, 619–663 (2010).
8. J. Karczmarek, J. Wright, P. Corkum, M. Ivanov, Optical centrifuge for molecules. *Phys. Rev. Lett.* **82**, 3420–3423 (1999).
9. D. M. Villeneuve, S. A. Aseyev, P. Dietrich, M. Spanner, M. Y. Ivanov, P. B. Corkum, Forced molecular rotation in an optical centrifuge. *Phys. Rev. Lett.* **85**, 542–545 (2000).
10. M. Spanner, M. Y. Ivanov, Angular trapping and rotational dissociation of a diatomic molecule in an optical centrifuge. *J. Chem. Phys.* **114**, 3456–3464 (2001).
11. L. Yuan, S. W. Teitelbaum, A. Robinson, A. S. Mullin, Dynamics of molecules in extreme rotational states. *Proc. Natl. Acad. Sci. U. S. A.* **108**, 6872–6877 (2011).
12. A. Korobenko, A. A. Milner, V. Milner, Direct observation, study, and control of molecular superrotors. *Phys. Rev. Lett.* **112**, 113004 (2014).
13. A. Korobenko, A. A. Milner, J. W. Hepburn, V. Milner, Rotational spectroscopy with an optical centrifuge. *Phys. Chem. Chem. Phys.* **16**, 4071–4076 (2014).
14. A. Korobenko, J. W. Hepburn, V. Milner, Observation of nondispersing classical-like molecular rotation. *Phys. Chem. Chem. Phys.* **17**, 951–956 (2015).
15. S. Fleischer, Y. Khodorkovsky, Y. Prior, I. S. Averbukh, Controlling the sense of molecular rotation. *New J. Phys.* **11**, 105039 (2009).
16. K. Kitano, H. Hasegawa, Y. Ohshima, Ultrafast angular momentum orientation by linearly polarized laser fields. *Phys. Rev. Lett.* **103**, 223002 (2009).
17. Y. Khodorkovsky, K. Kitano, H. Hasegawa, Y. Ohshima, I. S. Averbukh, Controlling the sense of molecular rotation: Classical versus quantum analysis. *Phys. Rev. A* **83**, 023423 (2011).
18. O. Korech, U. Steinitz, R. J. Gordon, I. S. Averbukh, Y. Prior, Observing molecular spinning via the rotational Doppler effect. *Nat. Photon.* **7**, 711–714 (2013).
19. K. Lin, Q. Song, X. Gong, Q. Ji, H. Pan, J. Ding, H. Zeng, J. Wu, Visualizing molecular unidirectional rotation. arXiv:1411.3523 (2014); *Phys. Rev. A*, in press (2015).
20. S. Zhdanovich, A. A. Milner, C. Bloomquist, J. Floß, I. S. Averbukh, J. W. Hepburn, V. Milner, Control of molecular rotation with a chiral train of ultrashort pulses. *Phys. Rev. Lett.* **107**, 243004 (2011).
21. C. Bloomquist, S. Zhdanovich, A. A. Milner, V. Milner, Directional spinning of molecules with sequences of femtosecond pulses. *Phys. Rev. A* **86**, 063413 (2012).
22. J. Floß, I. S. Averbukh, Molecular spinning by a chiral train of short laser pulses. *Phys. Rev. A* **86**, 063414 (2012).
23. B. J. Whitaker, *Imaging in Molecular Dynamics* (Cambridge Univ. Press, New York, 2003).
24. I. V. Litvinyuk, K. F. Lee, P. W. Dooley, D. M. Rayner, D. M. Villeneuve, P. B. Corkum, Alignment-dependent strong field ionization of molecules. *Phys. Rev. Lett.* **90**, 233003 (2003).
25. J. Itatani, J. Levesque, D. Zeidler, H. Niikura, H. Pepin, J. C. Kieffer, P. B. Corkum, D. M. Villeneuve, Tomographic imaging of molecular orbitals. *Nature* **432**, 867–871 (2004).
26. T. Kanai, S. Minemoto, H. Sakai, Quantum interference during high-order harmonic generation from aligned molecules. *Nature* **435**, 470–474 (2005).
27. R. Torres, N. Kajumba, J. G. Underwood, J. S. Robinson, S. Baker, J. W. G. Tisch, R. de Nalda, W. A. Bryan, R. Velotta, C. Altucci, I. C. E. Turcu, J. P. Marangos, Probing orbital structure of polyatomic molecules by high-order harmonic generation. *Phys. Rev. Lett.* **98**, 203007 (2007).
28. M. Meckel, D. Comtois, D. Zeidler, A. Staudte, D. Pavičić, H. C. Bandulet, H. Pépin, J. C. Keffer, R. Dörner, D. M. Villeneuve, P. B. Corkum, Laser-induced electron tunneling and diffraction. *Science* **320**, 1478–1482 (2008).
29. A.-T. Le, R. R. Lucchese, M. T. Lee, C. D. Lin, Probing molecular frame photoionization via laser generated high-order harmonics from aligned molecules. *Phys. Rev. Lett.* **102**, 203001 (2009).
30. H. Akagi, T. Kasajima, T. Kumada, R. Itakura, A. Yokoyama, H. Hasegawa, Y. Ohshima, Isotope-selective ionization utilizing molecular alignment and non-resonant multiphoton ionization. *Appl. Phys. B* **109**, 75–80 (2012).
31. M. Spanner, E. A. Shapiro, M. Ivanov, Coherent control of rotational wave-packet dynamics via fractional revivals. *Phys. Rev. Lett.* **92**, 093001 (2004).
32. K. F. Lee, D. M. Villeneuve, P. B. Corkum, E. A. Shapiro, Phase control of rotational wave packets and quantum information. *Phys. Rev. Lett.* **93**, 233601 (2004).
33. K. F. Lee, E. A. Shapiro, D. M. Villeneuve, P. B. Corkum, Coherent creation and annihilation of rotational wave packets in incoherent ensembles. *Phys. Rev. A* **73**, 033403 (2006).

34. J. P. Cryan, J. M. Glownia, D. W. Broege, Y. Ma, P. H. Bucksbaum, Ensemble of linear molecules in nondispersing rotational quantum states: A molecular stopwatch. *Phys. Rev. X* **1**, 011002 (2011).
35. A. G. York, Laser-driven clockwise molecular rotation for a transient spinning waveplate. *Opt. Express* **17**, 13671–13676 (2009).
36. U. Steinitz, Y. Prior, I. S. Averbukh, Optics of a gas of coherently spinning molecules. *Phys. Rev. Lett.* **112**, 013004 (2014).
37. H. Hasegawa, Y. Ohshima, Quantum state reconstruction of a rotational wave packet created by a nonresonant intense femtosecond laser field. *Phys. Rev. Lett.* **101**, 053002 (2008).
38. A. S. Mouritzen, K. Molmer, Quantum state tomography of molecular rotation. *J. Chem. Phys.* **124**, 244311 (2006).
39. A. Hishikawa, A. Iwamae, K. Hoshina, M. Kono, K. Yamanouchi, Coulomb explosion dynamics of N_2 in intense laser field by mass-resolved momentum imaging. *Chem. Phys.* **231**, 315–329 (1998).

Acknowledgments: We thank N. Mizutani, T. Toyoda, and the other members of the Equipment Development Center of the Institute for Molecular Science (IMS) for their support in constructing the imaging apparatus including electronics systems. Part of the calculations was performed at the Research Center for Computational Science, Okazaki, Japan. **Funding:** This work was supported in part by grants-in-aid from Japan Society for the Promotion of Science (JSPS) and Ministry of Education, Culture, Sports, Science and Technology (MEXT) Japan (#20050032, #22018031, #22245004, #26104539, #26620020, #26810011, and #15H03766); the Imaging Science Project of the Center for Novel Science Initiatives (CNSI), National Institutes of Natural Sciences (NINS) (#IS261006); the RIKEN-IMS joint program on "Extreme Photonics"; and Consortium for Photon Science and Technology. **Author contributions:** All authors designed the experiment, analyzed the data, and discussed the results. K.M. created the concept of the new ion-imaging setup, constructed the apparatus, and carried out the measurements. K.M. and Y.O. prepared the manuscript, and all authors commented on the manuscript. Y.O. supervised the project. **Competing interests:** The authors declare that they have no competing interests.

Submitted 7 December 2014
Accepted 19 May 2015
Published 3 July 2015
10.1126/sciadv.1400185

Citation: K. Mizuse, K. Kitano, H. Hasegawa, Y. Ohshima, Quantum unidirectional rotation directly imaged with molecules. *Sci. Adv.* **1**, e1400185 (2015).